

# Temporal Variation of Low-Latitude Zonal Circulations

PETER J. WEBSTER<sup>1</sup>—*Department of Meteorology, University of California, Los Angeles, Calif.*

**ABSTRACT**—The response of the tropical atmosphere to steady forcing for all four seasons is computed using a simple two-layer linear primitive-equation model allowing an arbitrary basic flow with two-dimensional shear. The character of each seasonal response is studied, and two distinct forms of behavior are found. Near the Equator, the forcing excites a slowly varying Kelvin wave of the time scale of months while, in midlatitudes, the atmosphere responds via the Rossby mode. Both regimes are separated by the critical latitudes existing on the poleward limits of the easterly channel of the basic flow. The long-wave scale response of the equatorial motions noted by Krishnamurti are shown to be the results of the natural filtering of the slowly varying Kelvin wave. The temporal variation of this zonal circulation is discussed.

The analysis is extended to infer the behavior and location of transient disturbances in the upper tropical tropo-

sphere for time scales much less than seasonal. Also shown is that the zonal mean flow plus the standing eddies are locally barotropically unstable, providing preferred geographical locations for the development and maintenance of transient disturbances. Such locations are shown to vary seasonally.

Variations of the tropical atmosphere of time scales much greater than seasonal also are investigated. It is shown that the correlations of Walker may be thought of as long-term variations in the seasonal standing eddies, which themselves provide a mode of communication throughout the tropical atmosphere. Also suggested is that the Walker circulation of the tropical Pacific Ocean may be thought of as the slowly varying filtered Kelvin wave response, within the easterly channel of the basic flow, weighted toward the long-wave heating distribution of low latitudes.

## 1. INTRODUCTION

The tropical atmosphere is seen to possess a near-complete gamut of spatial and temporal variation, with a range that encompasses the short lived small-scale individual cumulus cloud and variations of the annual cycle itself. Within these limits lie the short-period cloud clusters and transient disturbances and hurricanes that, together with the steady response of the tropical atmosphere to stationary heating and orography, constitute the various average seasonal circulations, each differing because of the position of the Sun and the relative location of the continents and oceans.

In recent studies [Webster 1972, 1973 (hereafter referred to as W1 and W2)], the dynamics of low latitude large-scale motions of time scales of the order of months have been theoretically investigated. Both studies use observed mean zonal winds to define a basic state for a simple linear and spherical two-layer primitive equation model, which was driven by realistic heating and orography functions distributed through the Tropics (local forcing). In the second study, the effect of forcing from higher latitudes (remote forcing) was included. It was concluded that the latent heating was responsible for most of the response near the Equator, but orography and remote effects became more important in the subtropics. The seasonal response of the December, January, and February (DJF) and June, July, and August (JJA) basic fields were calculated; and the results were compared with

observed low-latitude fields (Kidson 1968, Kidson et al. 1969, Krishnamurti 1971b) and with the results of more elaborate and complicated general circulation models (Manabe et al. 1970). Generally, the simple model was able to simulate at least the gross features of the low-latitude circulation, and the differences found in subtropical latitudes (W1) were minimized by including the effects of remote forcing (W2).

An interesting observation of the results of the studies is the manner in which the perturbation velocity response (i.e., the velocity field after subtraction of the zonal velocity) becomes progressively more zonal with decreasing latitude. This may be seen in figure 8 where the ratios between the computed 250-mb zonal and meridional perturbation velocity components for each season are plotted as a function of latitude. Figure 8 suggests that the flow becomes progressively confined to the latitude height plane as the Equator is approached. Poleward, the meridional velocity component becomes larger, and the forced flow assumes the characteristic wavelike appearance as the effect of rotation increases.

A possible explanation may be that the heating or forcing gradient may be so aligned that the response, down the gradient because of the small rotation effect, is in the zonal component. Such a simple explanation is rendered questionable by an examination of the heating fields (fig. 1), which show that appreciable meridional heating gradients exist across the Equator. One of the major aims of this paper is to understand the low-latitude zonal response to forcing functions that need not be aligned zonally.

<sup>1</sup> Now with the Department of Atmospheric Sciences, University of Washington, Seattle, Wash.

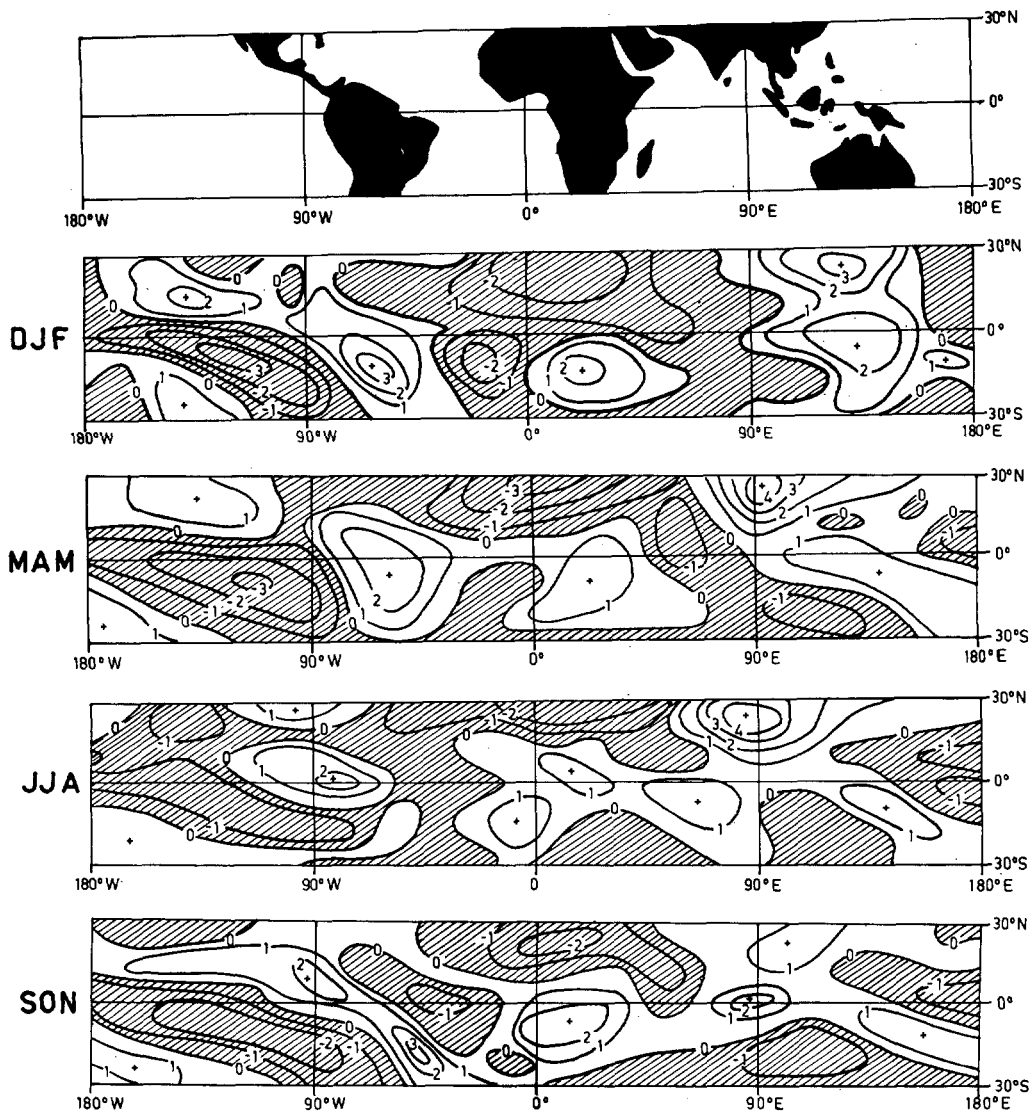


FIGURE 1.—Seasonal distributions of the perturbation heating ( $10^2 \text{ cal} \cdot \text{cm}^{-2} \cdot \text{day}^{-1}$ ) due to latent heat release in the tropical atmosphere. The hatched areas denote regions of relative cooling.

Such questions have been raised, at least implicitly, for many years. For example, Walker (1923), in a statistical investigation of the long-term variation of the atmosphere, found that there were strong correlations between low-latitude station pairs for various physical parameters. A general review of the many papers of Walker is given by Montgomery (1940). Troup (1965) substantiated these correlations using longer periods of data. These correlations and their geographic location strongly suggest a form of atmospheric teleconnections and the possibility of some form of slowly varying zonal circulation at low latitudes. Bjerknes (1969) has drawn particular attention to the temporal variation of the zonal asymmetries with emphasis on the Walker circulation, a name ascribed to the equatorial thermodynamically direct circulation ascending in the western Pacific Ocean and Indonesia and descending in the eastern Pacific. An important aim of this paper is to define the physical nature of these long term low-latitude variations.

Krishnamurti (1971a, 1971b) has made an extensive observational analysis of the mean circulation of the tropical troposphere using data for the Northern Hemisphere summer of 1967. Besides using the conventional network of radiosonde and rawinsonde stations, Krishnamurti was able to supplement them with a large number of commercial aircraft reports. (Fig. 1.4 in Krishnamurti 1971b indicates the flight paths of these aircraft.) Supplemental data provide some additional information of the flow in the data-sparse northern equatorial Atlantic Ocean and the western equatorial Pacific Ocean. However, the very low latitudes and most of the Southern Hemisphere, especially in the Atlantic and Indian Ocean and the southern and eastern regions of the Pacific, still remain relatively data deserts. Krishnamurti (1971a) concentrates on the existence and definition of low-latitude zonal (east-west) circulations in the low latitudes for the 1967 summer. His observations suggest that the upper level flow in the Northern Hemisphere is dominated by the outflow as-

sociated with the Indian monsoon system. Besides this dominating feature, Krishnamurti shows a number of lesser circulations and suggests that the Walker circulation of Bjerknæs (1969) is merely a southern extension of this major circulation. The definition of this circulation, its physical nature, and the annual variation of similar low-latitude circulations is an important consideration of this paper.

Then, there are three major reasons for making this further study of the zonally asymmetric quasi-stationary motions of the tropical atmosphere. The first is to extend the analysis of the low-latitude circulations to a complete year and determine if the zonal circulations sensed by Walker (1923) and noted by Bjerknæs (1969) and Krishnamurti (1971a) are apparent in other seasons besides the Northern Hemisphere summer and investigate their physical nature. The second is to see if it is possible to infer the nature of shorter time-scale variations from the seasonal mean fields. The third reason is to determine why Walker (1923) and Troup (1965) found correlations between various station pairs using long periods of data.

Specifically, we will use the simple model detailed in both W1 and W2 to study the low-latitude circulations for the four seasons DJF, March through May (MAM), JJA, and September through November (SON). From the response of the seasonal basic fields to specific seasonal forcing, we will study the variation of the intensity and position of the low-latitude circulations and attempt to determine their physical nature. Using the computed seasonal average circulations, we shall make inferences regarding both the short- and long-term variations of the response.

## 2. SEASONAL FORCING FUNCTIONS

In this study, the model will be driven in an identical manner to that in W1 and W2. Since the effect of sensible and direct radiational heating were shown to be relatively unimportant functions compared to the effect of latent heat advection by the atmosphere, they will once again be neglected. Thus, only the effect of orography and latent heating will be considered.

Although the release of latent heat is very large, it is really a secondary effect because this form of heating is completely dependent, at least initially, upon other factors or forcing to provide the necessary phase change. For example, the effect of sensible heating of a column of air may initiate the liberation of large amounts of latent heat. However, because of the very simple model we consider here, the gross simplification of the hydrology cycle requires that we treat the latent heating as some known function.

The distribution of latent heat in the tropical atmosphere is determined in an identical manner to that in W1. Because of the scarcity of data in the Tropics, especially over the vast ocean regions, the determination of the function using precipitation data is unsatisfactory. To overcome this, we devised an alternative method that shows a

minimum of bias between continental and oceanic regions. The following is an outline of the implicit scheme:

1. From the global time-averaged satellite brightness or visual albedo mosaics (Taylor and Winston 1968), an estimate of the seasonal cloud cover was made over tropical latitudes. These distributions were modified by subtracting out bright cloudless areas over deserts by using climatological precipitation data. Such regions were relegated to the lowest brightness (and so cloudiness) index.

2. The zonal mean brightness of cloudiness was then correlated with a zonal mean latent heat determination made using precipitation data. In this case, the Northern Hemisphere latent heat estimates for January and July from Katayama (1964) were used. The correlation provides a factor of proportionality between the cloudiness and latent heat release. This means that an error in Katayama's explicit determination leads only to an error in the magnitude, but not the distribution, of our implicit estimation.

3. Multiplication by the proportionality factor and subtraction of the zonal mean from the cloudiness charts yield the spatial deviations of the latent heat fields.

The resultant fields are shown in figure 1. One can see that, generally, the heating areas (positive) are associated with the equatorial continents (Central America and Brazil, Equatorial Africa and Indonesia, and Southeast Asia); whereas the relative cooling regions (negative and cross-hatched) correspond to ocean regions. The most intense and largest oceanic cooling region appears over the equatorial and southeastern Pacific Ocean, being strongest in DJF and MAM and weakest in JJA. Contrary to the above rule, relative heating takes place over the Indian Ocean in both JJA and SON and persistently in all seasons in a band stretching from the northwest to the southeast in the South Pacific Ocean. Anomalous cooling regions also exist over the arid continental regions of North Africa and the Middle East with magnitudes comparable to the oceanic cooling regions. The heating fields for both MAM and JJA are dominated by positive heating in the regions of Central America and Brazil in the Western Hemisphere and over the Indian region in the Eastern Hemisphere. The major heating in DJF occurs in Brazil and in Southeast Asia and Indonesia. Except for considerably weaker heating in the Far East, SON is similar to the DJF distribution.

The implicit method just described requires the use of the basic assumption that there is a relationship between cloudiness and precipitation (and therefore with latent heat release). Whereas this appears to be a rather weak assertion, it is perhaps stronger in the tropical atmosphere than elsewhere because of the predominance of cumulus-type cloud. To test the assumption, W1 compared regions of relatively well-known precipitation with the inferred precipitation distributions obtained from the latent heat fields. The agreement was fair. In any event, it seems that this method provides at least a consistent estimate of the latent heat release in the data-sparse Tropics.

In addition to the heating fields, the model allows the interaction of the basic fields with orography that is prescribed at the lower boundary. The form is the same

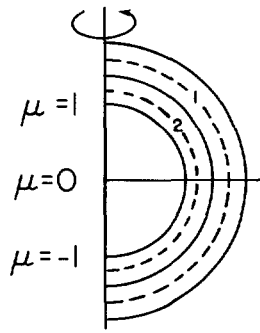


FIGURE 2.—Schematic representation of the two-layer spherical model.

as that used in W1 and W2 and can be seen in figure 2A of the first paper.

### 3. SEASONAL RESPONSE

The response of the tropical atmosphere to the seasonal heating distributions and orography, discussed in section 2, will be examined with the aid of the simple model developed in W1 and W2. Since the details of the model are discussed in both papers, only a brief outline is given here.

The model is a linear two-layer formulation of the hydrostatic primitive equations of motion in spherical pressure coordinates. The domain of the model extends from pole to pole and includes simple linear dissipation laws, which represent surface friction, turbulent exchange of momentum in the vertical, and radiative cooling. The model was constructed to determine the response of an arbitrary basic zonal flow to a known set of forcing functions. The two-layer model is represented schematically in figure 2; and the response of the basic flow,  $U(\theta, p)$ , is given by the horizontal components of the velocity vector ( $u$  is the eastward component, and  $v$  is the northerly component) and the geopotential,  $\phi$ , at the middle levels of each layer (750 and 250 mb) and the vertical velocity,  $\omega$ , at their interface (500 mb).

The four seasonal distributions of the basic zonal velocity,  $U$ , are shown in figure 3. Each curve is characterized by strong westerlies in the subtropics and middle latitudes, which are most intense in the winter hemispheres. At low latitudes, easterlies dominate both the upper and lower troposphere, although extending more poleward in the lower levels. In W2, we pointed out that the zeros of the basic zonal flow represent the critical latitudes of the stationary forced modes. At these latitudes, the phase speed of the stationary waves is identical to the basic flow. For reference, these latitudes are listed in table 1.

From the character of the forcing functions and the complexity of the basic zonal flow, it is apparent that the model may respond in a complicated and varied manner from season to season. To illustrate this variation, we show the derived stream function,  $\psi$ , in figure 4 and the velocity potential,  $\chi$ , in figure 5.

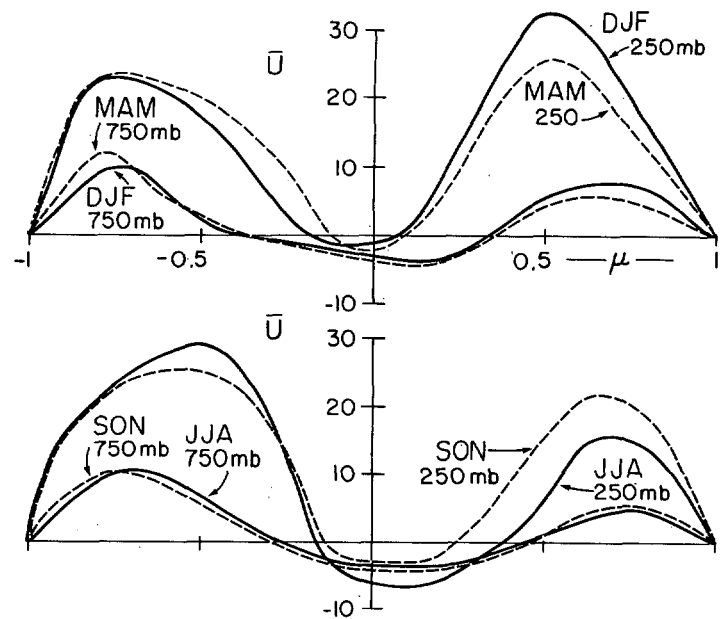


FIGURE 3.—Basic zonal wind,  $U$  (m/s), for each season as a function of latitude for the two levels of the numerical model.

TABLE 1.—Seasonal variation of the critical latitudes for stationary modes, corresponding to the zeros of the basic zonal current,  $U(\theta, p)$ , shown in figure 3

Season		250 mb		750 mb	
DJF	$\mu_c$	-0.2	0.05	-0.45	0.35
	$\varphi_c$	-11.5°	2.9°	-26.7°	20.5°
MAM	$\mu_c$	-0.1	0.05	-0.4	0.4
	$\varphi_c$	-5.7°	2.9°	-23.6°	23.6°
JJA	$\mu_c$	-0.15	0.35	-0.3	0.45
	$\varphi_c$	-8.6°	20.5°	-17.5°	26.7°
SON	$\mu_c$	-0.1	0.2	-0.4	0.45
	$\varphi_c$	-5.7°	11.5°	-23.6°	26.7°

### Fields of Stream Function

The fields of the rotational part of the flow were calculated from the velocity fields for a closed channel bordered at  $\theta = \pm 45^\circ$  where it was insisted that the stream function remains zero. Specifically, the stream function was determined by relaxation of the Poisson equation defined by the derived vorticity field

$$\mathbf{k} \cdot \nabla \times \mathbf{V} = \nabla^2 \psi = \frac{1}{\cos \theta} \left[ \frac{\partial}{\partial \theta} (u \cos \theta) - \frac{\partial v}{\partial \varphi} \right] \quad (1)$$

where  $\nabla^2$  is the two-dimensional spherical Laplacian,  $\theta$  is latitude, and  $\varphi$  is longitude. The most dominating and persistent feature for all seasons, except SON, is the strong anticyclonic system (having a southwest to northeast orientation and extending westward from the western Pacific Ocean region, across the African Continent to the western Atlantic Ocean). This anticyclone is coupled with a cyclonic circulation over the northern Atlantic Ocean (fig. 4). On the equatorward side of the anticyclone is the persistent easterly stream (the easterly

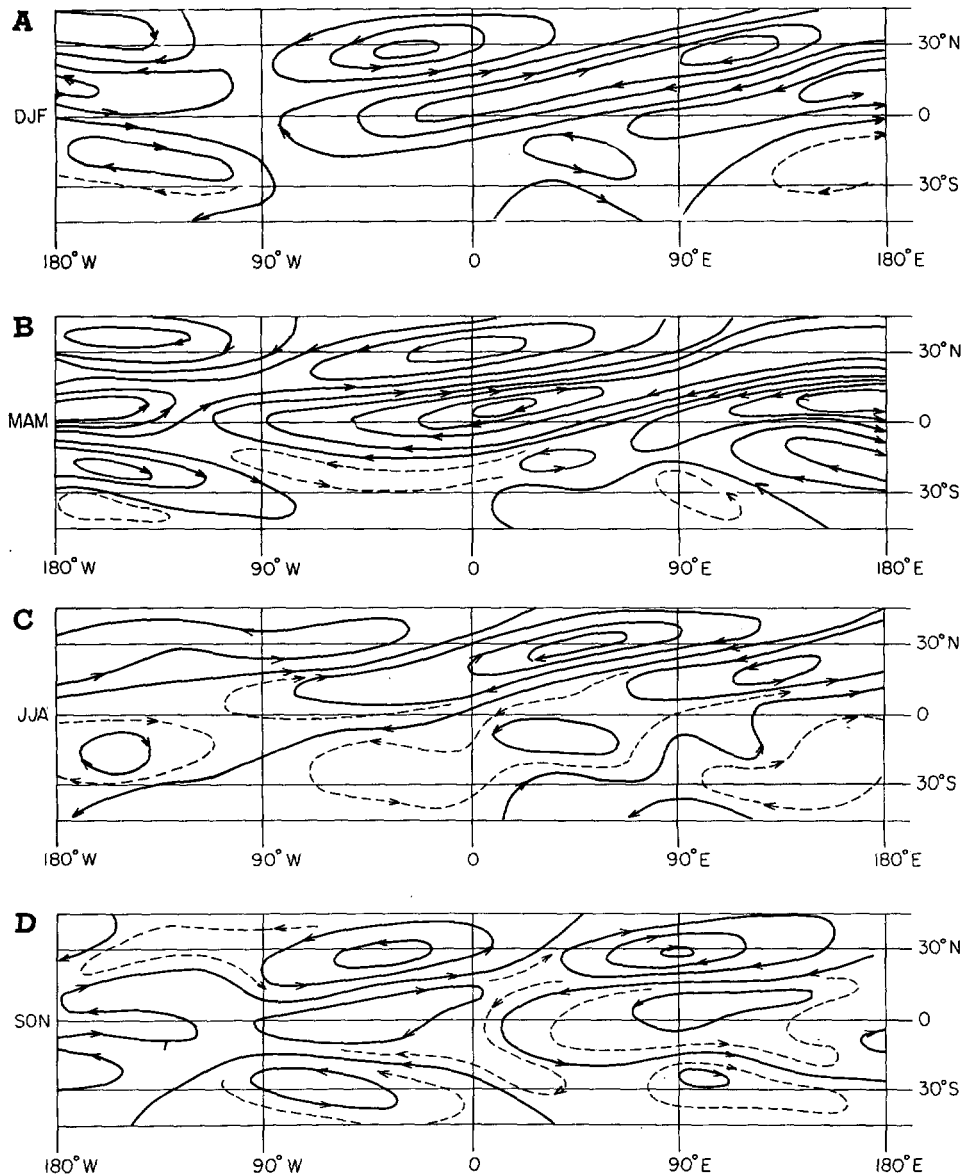


FIGURE 4.—Distribution of the stream function,  $\psi$  ( $10^{-5}\text{m}^2\text{s}^{-1}$ ), for (A) DJF, (B) MAM, (C) JJA, and (D) SON. The isolines are drawn every 50 units, and the dashed curves are intermediate isopleths.

jet), which is both highly variable in position and intensity. In DJF and MAM, the easterly maximum is intense and confined to low latitudes. In MAM, there appears to be the development of a two-cell system with an anticyclonic circulation positioned over Africa near the prime meridian and the Equator. Strong westerlies prevail on the poleward side of the anticyclone over North Africa and India. In JJA, the anticyclone appears to have moved westward, and the easterly maximum has replaced the strong perturbation westerlies over India while the North Atlantic cyclone has weakened and moved to the west. SON is characterized by a generally weaker circulation that was anticipated from figure 1, which shows that the magnitude of the heating is less than that for other seasons. Over the Indian region, the anticyclone has weakened and again has moved east and south; in the Atlantic, the cyclonic flow has been re-established. SON appears as a period of transition between

the Northern Hemisphere summer and winter circulation systems.

### Fields of Velocity Potential

The velocity potential,  $\chi$ , was calculated for each season by relaxation of the derived divergence fields; that is,

$$\nabla \cdot \mathbf{V} = \nabla^2 \chi = \frac{1}{\cos \theta} \left[ \frac{\partial u}{\partial \phi} + \frac{\partial}{\partial \theta} (v \sin \theta) \right] \quad (2)$$

where the velocity potential is set to zero at the lateral boundaries. By use of the continuity equation expressed at the mid-level of the two-level model, the vertical velocity field is implicit in the velocity potential field as

$$\begin{aligned} \omega &= -\frac{1}{\cos \theta} \nabla \cdot \mathbf{V}_{250 \text{ mb}} = -\frac{1}{2} \nabla \cdot (\mathbf{k} \times \nabla \psi + \nabla \chi) \\ &= -\frac{1}{2} \nabla^2 \chi = -\frac{1}{2} \nabla^2 V_x. \end{aligned} \quad (3)$$

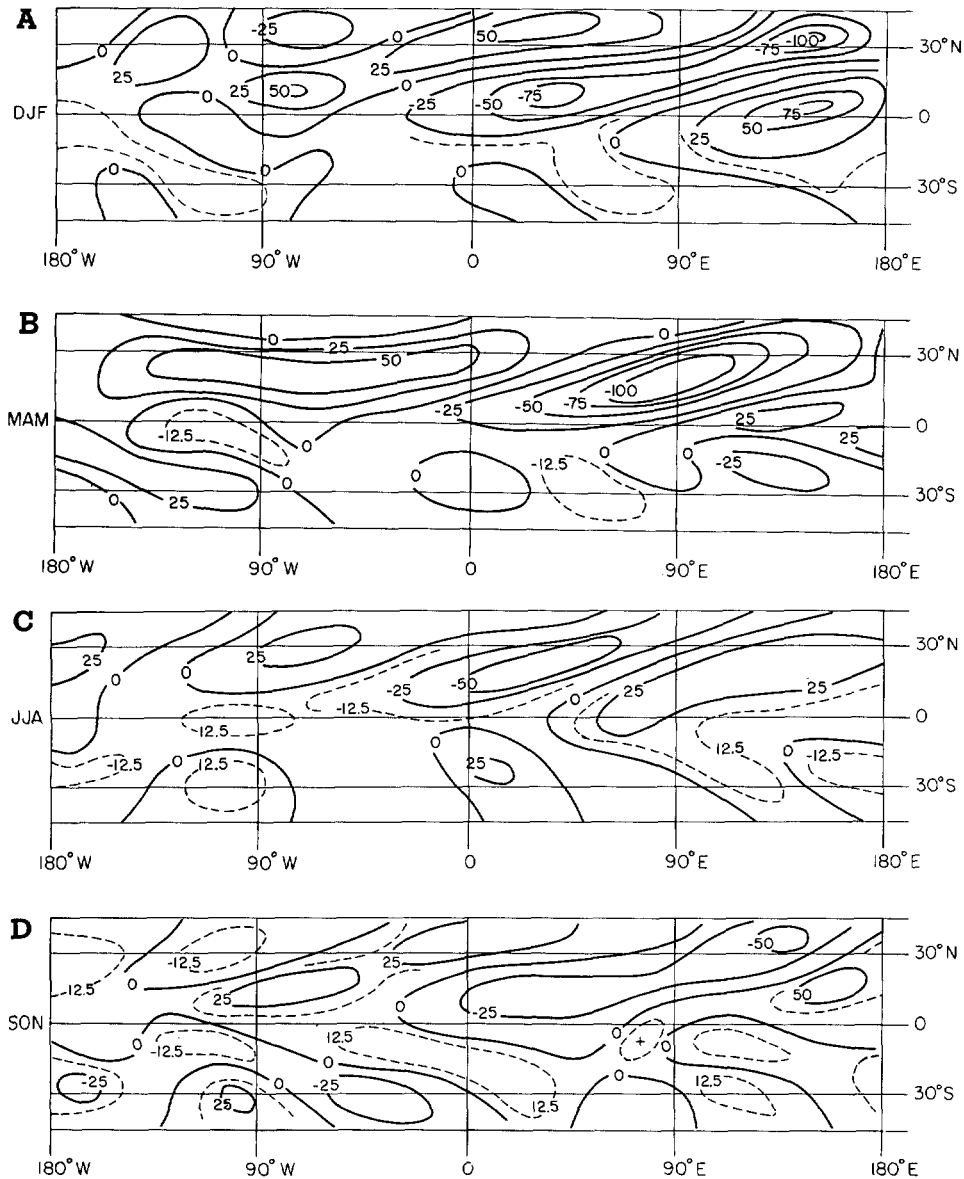


FIGURE 5.—Same as figure 4 except this is for the velocity potential. The negative values indicate the mean ascending motion.

Thus centers of negative velocity potential correspond to regions of mean ascending motion, and positive values refer to descending motion. The divergent part of the velocity field is parallel to the gradient of the velocity potential such that negative regions correspond to regions of outflow, and vice versa, which is consistent with eq (3).

As with the fields of stream function, the major features of the velocity potential occur in the eastern part of the Northern Hemisphere (fig. 5). The seasonal fields for DJF and MAM indicate strong outflow regions in similar locations to the anticyclonic circulation shown in figures 4A and 4B. The major difference is the splitting of the maximum outflow in DJF to yield divergence centers over Equatorial Africa and the northwestern Pacific Ocean. In JJA, the divergent region moves north and west to lie over and to the west of the Indian subcontinent. Other features are the persistent convergent regions in the southwestern Pacific and the positive areas dominating the western part of the Northern Hemisphere

in most seasons. The character of these features and their relationship to the forcing will be considered in section 4.

### Spectral Form of the Response

To ascertain the scale dependence of the response of the model Tropics is important. To accomplish this, we plotted the power of the kinetic energy at 250 mb for each longitudinal wave number,  $s$  (in the upper bars of fig. 6), for each season and five latitude bands. The kinetic energy of the perturbations is shown as a percentage of the zonal average of the total perturbation kinetic energy for that latitude circle shown on each diagram. The lower bars (shaded) represent a corresponding spectral breakdown of the latent heat forcing distributions presented in figure 1. The most interesting feature may be seen at 15°N and the Equator where most of the energy appears to reside in the low wave number end of the spectrum. For example, along the Equator in DJF, MAM, and

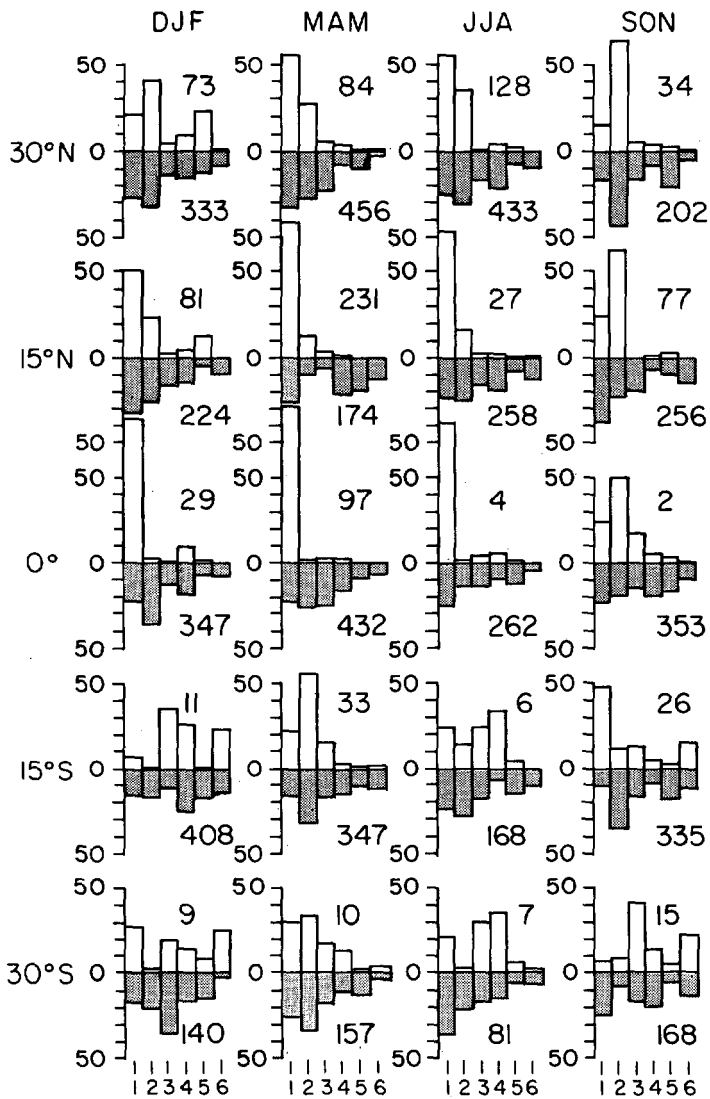


FIGURE 6.—Distribution of the power of the kinetic energy response ( $\text{m}^2\text{s}^{-2}$ , upper bars) and the forcing due to heating ( $\text{cal}\cdot\text{cm}^{-2}\cdot\text{day}^{-1}$ , lower shaded bars) plotted for various latitudes and for each season as a function of longitudinal wave number,  $s$ . The bars represent the contribution (in percent) of the total quantity shown on each diagram for each wave number.

JJA, more than 80 percent of the kinetic energy can be attributed to  $s=1$ . Farther north, the energy is spread over a larger spectral range but is generally restricted to  $s=1$  and 2; in the Southern Hemisphere, the little perturbation energy produced by the forcing is also more evenly distributed over the spectral range. Note that the total perturbation kinetic energy produced in the Northern Hemisphere is nearly an order of magnitude greater than that in the Southern Hemisphere.

The spectral power of the heating shown in the lower bars of figure 6 provides a more even distribution over the first six wave numbers of the longitudinal expansion. Whereas one might expect a one-to-one spectral relationship between the kinetic energy and the forcing, it is apparent that such an agreement does not occur at all latitudes. Near the Equator, the large  $s=1$  kinetic energy response of the model does not mirror the forcing distribution, indicating that a more complicated relation-

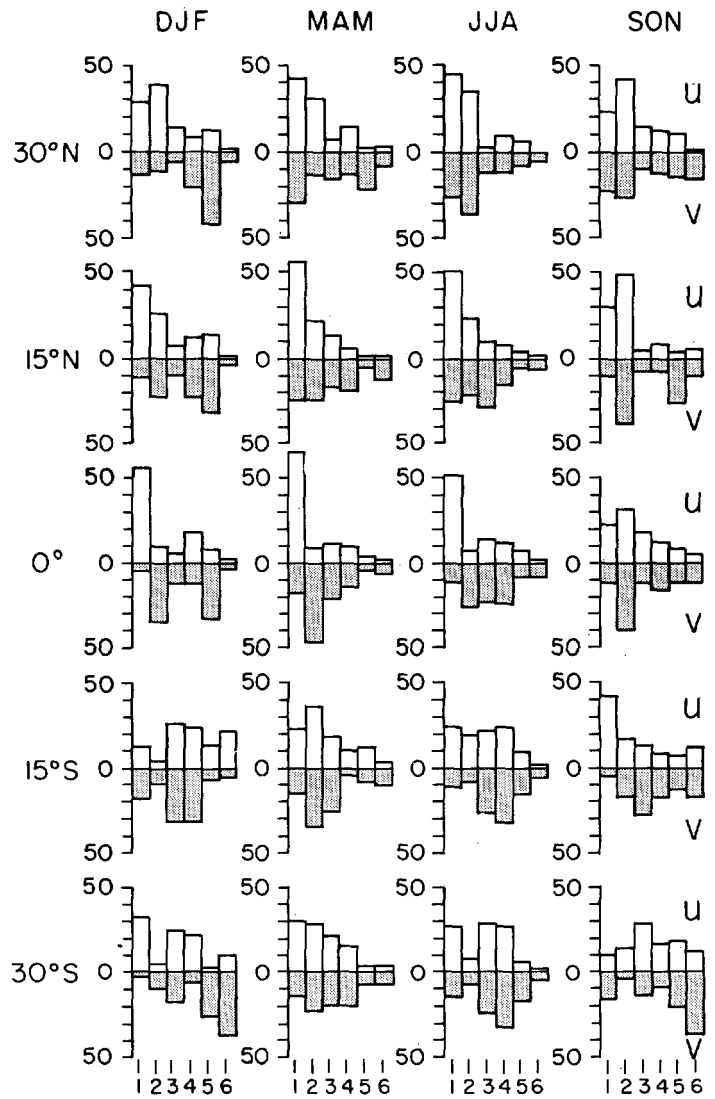


FIGURE 7.—Same as figure 6 except this is the spectral distribution of the perturbation velocity components,  $u$  (upper bars) and  $v$  (lower shaded bars).

ship exists near the Equator. At higher latitudes, the resemblance between the forcing and the response increases. In section 4, we show that the spectral response to a particular heating distribution is both a function of latitude and the sign of the basic current—in other words, determined by the modal form of the response.

Figure 7 depicts the corresponding breakdown of the perturbation velocity components. The upper bars show the spectral distribution (in percent) of the zonal perturbation velocity response for each season while the corresponding distribution for the meridional component is shown in the lower half of each diagram (shaded). Two general features emerge from this figure. First, the spectral form of  $u$  is confined to the longest modes (especially near the Equator) while, at 30°S, the response is more general. The  $u$  spectra at low latitudes conform well to the kinetic energy spectra. Second, the  $v$  spectra at all latitudes and seasons are distributed more widely in  $s$  than the  $u$  component and do not exhibit its low wave-number response at low latitudes. Note that the

JJA spectral distribution tends to agree fairly well with Krishnamurti's (1971b) observations for the 1967 Northern Hemisphere summer.

#### 4. CHARACTER OF THE RESPONSE

The salient features of the seasonal response, as indicated by figures 4-7, allow us to define the physical character of the response. These features may be summarized as follows:

1. A large variation occurred (from season to season) both in the form and position of the model response. Much of this may be attributed to the seasonal variation of forcing, but the large variations in the stream function and velocity potential with latitude for similar forms of forcing suggest different modal response with latitude.

2. The spectral form of the kinetic energy response also differs markedly, especially as a function of latitude. In general, at low latitudes, the response occurs at the low wave number end of the spectrum and more generally spreads over the spectrum at higher latitudes. Little correlation with the form of the forcing at low latitudes with the forcing is apparent.

3. The power spectra of the zonal component of the perturbation velocity appears to follow the kinetic energy spectra at low latitudes. The  $v$  spectra, on the other hand, are spread through the spectra.

In figure 8, the relative magnitudes of the perturbation  $u$  and  $v$  fields are shown as a function of latitude for each season. The ordinate plots the ratio of the absolute values of  $u$  and  $v$  against latitude for 250 mb, as given by the expression

$$X = (\Sigma|v|/\Sigma|u|)_{250\text{mb}}. \quad (4)$$

Two regimes of  $X$  are evident, each denoted by values of either 0(1) or 0(1/10). Generally, the response in very low latitudes is nearly all in the zonal component; but in the subtropics, the response is nearly equal for both components. This allows us to reinterpret the kinetic energy spectra (fig. 6) as being mainly a function of the zonal velocity component of low latitudes, as we had inferred from the similarity of the  $u$  spectra shown in figure 7. The inference is that the  $v$  spectra of figure 7 represent very little power with decreasing latitude but nearly equal power at higher latitudes.

The shaded region represents the extent of the easterlies of the basic fields shown in figure 3. The northerly and southerly boundaries of this equatorial channel are the critical latitudes for the stationary forced waves at 250 mb as discussed in W2. In this paper, it was shown that only a small amount of wave energy could propagate into the easterly channel in a dissipative system from the higher latitude westerly region. In this manner, the easterlies act as an effective barrier to subtropical influence. Therefore, any indicated response within the easterlies must result from local forcing within that channel. In noting the change of  $X$  between the easterlies and the westerlies, remember that the basic state possesses both vertical and horizontal shear, which must be taken into account in calculating the critical latitude of the model. That is, each layer possesses its own critical latitude because of the

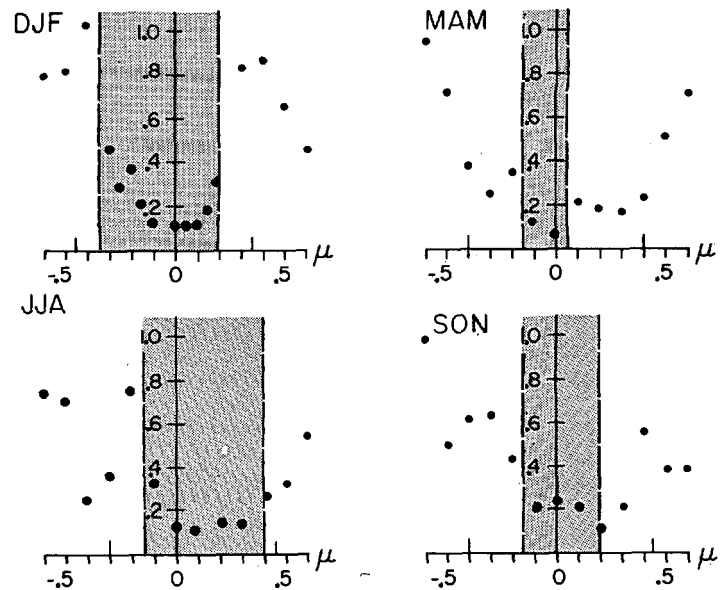


FIGURE 8.—Ratio ( $\Sigma|v|/\Sigma|u|$ ) of the total power of the perturbation components shown as a function of latitude for each season at 250 mb. The shaded region within the dashed lines represents the easterly channel of the basic flow.

vertical shear. Those of the lower level are indicated by the bars on the axis of figure 8. The effect of vertical shear plus the variation of dissipative effects in each layer probably cause the slightly more complicated distribution of  $X$  than would be expected from merely horizontal shear. These features are discussed in W2.

From figure 8, we see that the easterlies are regions of small  $X$ ; regions poleward of the easterlies possess larger values. This infers that different modes are excited within and without the channel with little or no communication between the two regimes. The modes excited within the channel exhibit a near-zero energy contribution from the meridional components and a preferential response to the low wave number forcing. On the other hand, the response in the westerlies shows a more equal energy partition between the components.

In W1, it was shown that only two modes are capable of response to stationary forcing in an easterly basic current. The first is the eastward-moving Kelvin wave that (for a continually stratified, isothermal, and spherical atmosphere moving in solid rotation relative to the rotating Earth) possesses the horizontal eigen-solutions

$$\begin{aligned} w_s(\theta) &\propto \exp\left(\frac{-\eta^2}{2}\right), \\ v_s(\theta) &= 0, \\ u_s(\theta) &\propto s^{-1} \exp\left(\frac{-\eta^2}{2}\right), \end{aligned} \quad (5)$$

and

$$\psi_s(\theta) \propto s^{-1} E^{-1/2} \exp\left(\frac{-\eta^2}{2}\right)$$

where  $E$  is the eigenvalue given by

$$E = \frac{4}{\delta^2}$$

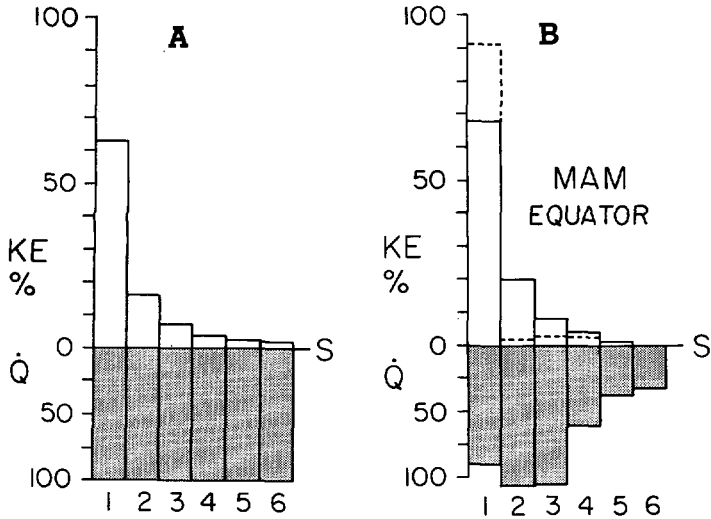


FIGURE 9.—Spectral distribution of the kinetic energy for the theoretical Kelvin wave response (A) to the white-noise forcing of  $100 \text{ cal}\cdot\text{cm}^{-2}\cdot\text{day}^{-1}$  and (B) to the equatorial latent heat distribution of MAM. The upper bars depict the kinetic energy (KE) response (in percent) of each wave number to the forcing distribution ( $\dot{Q}$ ) shown by the lower shaded bars. The dashed bars in (B) signify the actual model response shown in figure 6.

and 
$$\eta = (1 + \delta)^{1/2} E^{1/4} \cos \theta. \quad (6)$$

Here,  $\delta$  is a nondimensional quantity defined by the basic flow

$$U(\theta) = \delta a \Omega \cos \theta \quad (7)$$

where  $\delta < 0$  for  $U < 0$ .

Equation (5) gives the latitudinal variation of the Kelvin wave as a function of the longitudinal wave number  $s$ . The constants of proportionality are determined by the magnitude of the forcing at that wave number  $s$ , plus dimensional quantities. The second mode capable of excitation is a set of eastward-moving gravity waves, which were shown in W1 to propagate far quicker than the basic flow, providing only a small insignificant response trapped very close to the Equator. The Kelvin wave, however, has magnitude  $e$ -folding latitudes near  $8^\circ$  on either side of the Equator for a basic flow of order  $-5 \text{ m/s}$ .

The most important features of eq (5) are that the meridional velocity component of this simple atmosphere is zero and that the zonal component is inversely proportional to the wave number  $s$ . This means that the kinetic energy distribution in the region of Kelvin wave activation goes as the inverse square of the wave number; that is,

$$\frac{1}{2}(u^2 + v^2) \propto \frac{1}{s^2} \exp(-\eta^2). \quad (8)$$

Significantly, this means that, for a given forcing function with equal power in each wave number (i.e., white-noise forcing), the Kelvin wave will respond to the  $s=1$  forcing by more than a factor of 4 over an equal magnitude forcing at  $s=2$ . In this manner, the Kelvin wave acts as a natural filter to the small scale time-independent forcing in the easterlies, a feature reflected in the kinetic energy response spectra shown in figure 6. Examples of

this filtering are shown in figure 9. The relative response of the Kelvin wave to equal amplitude forcing is illustrated in figure 9A, showing the rapid decrease of response with increasing  $s$ . In figure 9B, the theoretical Kelvin response to MAM seasonal forcing along the Equator (as shown in fig. 1) is compared to the actual response of the model at 250 mb, which is denoted by dashed bars in the upper part of the diagram. The theoretical and derived responses are similar, although the latter possesses an even sharper short-wave cutoff.

In the subtropical and mid-latitude westerlies, two modes of oscillation are again excitable by stationary forcing. These are the westward-propagating Rossby waves and a set of gravity waves moving in the same direction. Little excitation of the second mode appears possible because of their relatively rapid phase propagation, which is over  $60 \text{ m/s}$  for such a model, whereas the basic flow does not exceed  $32 \text{ m/s}$  at any latitude. However, within the set of Rossby waves, there are modes that possess phase speeds which may match the basic flow and thus may be forced. Furthermore, the Rossby wave has the property of an equivalence in magnitude between the two horizontal velocity components, which strongly suggests that the model response poleward of the critical latitudes is in the Rossby mode. In this way, the subtropical kinetic energy spectrum is a function of both components.

In summary, the response of the two-layer dissipative model possessing two-dimensional basic shear may be explained, at least in part, by the modes of the simpler analytic model described in W1. Within the easterlies, much of the structure of the steady-state fields corresponds to that of the simple rotationally trapped Kelvin wave. Whereas the forcing fields possess gradients in arbitrary directions, most of the response is seen to be down and parallel to the latitudinal component of the heating gradient, a consequence of the mode forced and the Kelvin wave's vanishing meridional velocity component. The response at low latitudes then emerges as quasi-stationary zonal circulations with their rising regions coinciding with the major heating fields and their descending legs over the regions of relative cooling but with a strong bias toward very large scale forcing. Furthermore, because of the evenness of the Kelvin wave about the Equator, as suggested by eq (5), the resultant flow within the easterly channel may be thought of as a response to the latitudinal average heating across the channel, weighted with contributions nearer the Equator. The deviations between the simple Kelvin wave and the waves generated in this dissipative model with shear may be seen in the nonzero, although still small, values of  $X$  near the Equator in figure 8. In middle latitudes, the response appears to be of the Rossby type with the flow aligning itself perpendicular to the heating gradient and with both velocity components contributing equally to the kinetic energy distribution.

## 5. SHORTER TERM VARIATIONS

We emphasized in W1 and W2 that the seasonal stationary modes ascribe much of their characteristic fea-

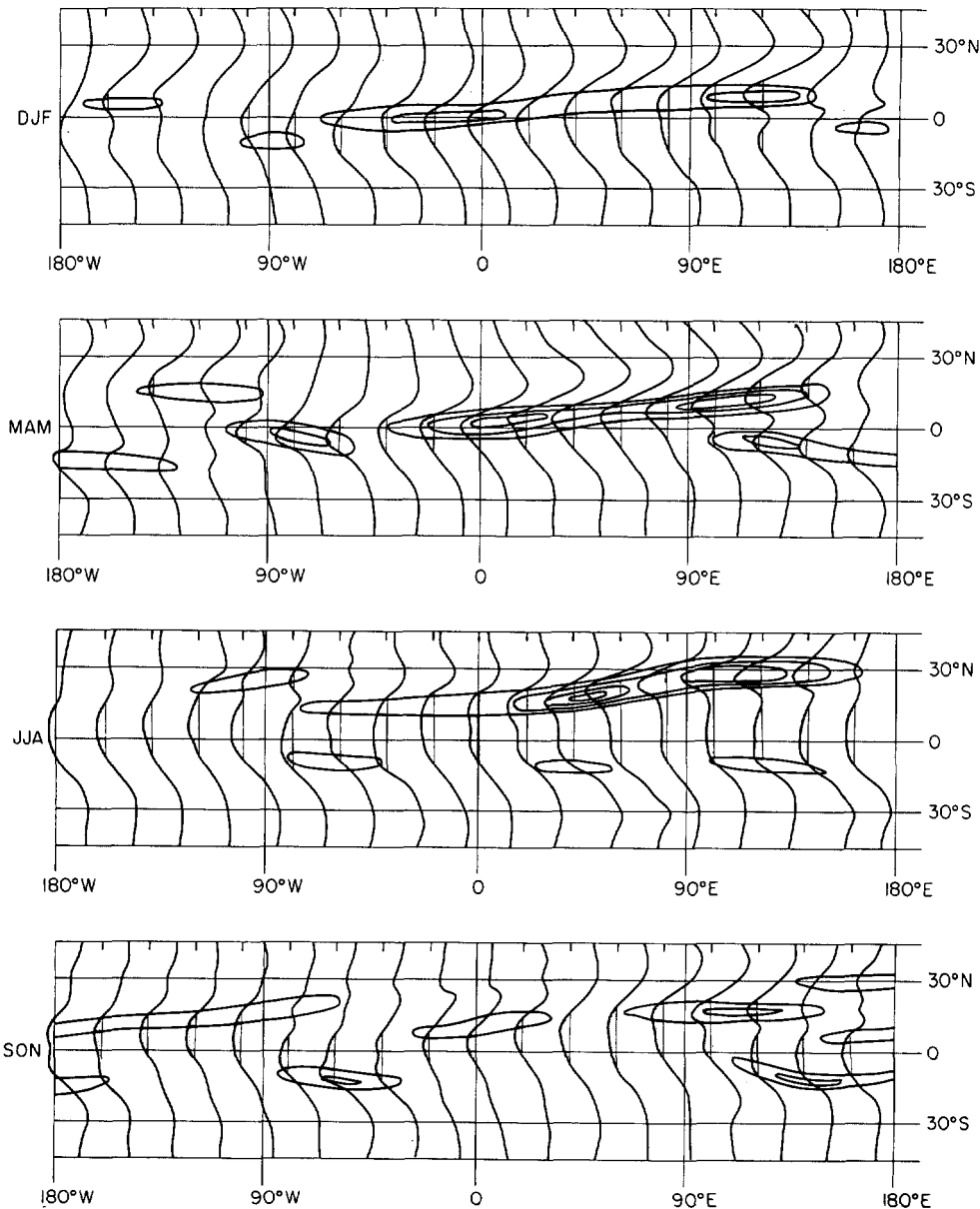


FIGURE 10.—Seasonal distribution of the total zonal wind component ( $u + U$ ). The shaded regions denote an easterly component, and the curves are relative to the marks on the upper axis. The distance between two successive marks represents 40 m/s. The closed isopleths, drawn at intervals of  $25 \times 10^{-12} \text{m}^{-1} \text{s}^{-1}$ , represent regions in which  $(\beta - u_v v) > 0$ .

tures to the low-latitude general circulation. For example, the easterly jet system of the Eastern Hemisphere may be considered a low wave number response to the latent heating distribution from the Indian Ocean and South-east Asian regions. Furthermore, these stationary features may be considered to be slowly varying, relative to the changing seasonal forcing field. Superimposed on these seasonal mean fields are smaller length and shorter time scale transient disturbances propagating through the upper troposphere. For example, Koteswaram and George (1958) indicate the propagation of such disturbances along the easterly jet stream from the western Pacific Ocean and over the Indian region. In addition, they noted periodic surges or oscillations in the strength of the easterly jet stream and were able to correlate variations in monsoon behavior with both phenomena. Understanding the energy sources of these disturbances is important.

The fact that the disturbances propagate along the easterly maximum and that there is some observed relation between the strength of the stream and the strength of the perturbation suggests that the forced seasonal waves and the transient waves may be physically coupled. The mechanism for this region was first suggested by Krishnamurti (1971a) who noted that the tilts of the ultralong seasonal waves and those of the shorter scale waves were oriented in such a manner that a barotropic interchange of energy between them was possible. In essence, the possibility of the large-scale flow being barotropically unstable was suggested. This theory was further advanced by Colton (1973) who, by the use of a simple barotropic model, considered the interaction of the transient and stationary modes. The driving of his model was accomplished using the observed divergence field at 200 mb for the Northern Hemisphere summer of 1967. Colton was

able to simulate the development of these small-scale disturbances in the western Pacific Ocean, their propagation over the Indian region, and the corresponding periodic surges in the basic flow.

Note that the mean zonal flow itself or the ultralong waves are both independently barotropically *stable*, and it is the sum of *both* (i.e., basic zonal flow and stationary waves) that is barotropically *unstable*. This was noted by Nitta and Yanai (1969) from a study of wave development in the central Pacific and also by Lorenz (1972) for the mid-latitude westerlies. Similarly, a study of the absolute vorticity of the basic flow for each season, as shown in figure 3, finds no latitude at which the stability criteria for a barotropic fluid,

$$(\beta - u_{yy}) > 0 \quad (9)$$

where  $\beta = 2\Omega \cos \theta/a$ , is encountered. Also, an investigation of the ultralong wave response relative to the forcing fields shown in figure 1 also yields only stable flow. However, a stability analysis of the perturbation field *plus* the zonal mean fields (an approximation representation of the highly nonlinear atmosphere with interacting zonal and perturbation quantities) shows regions of barotropic instability. The zonal velocity component in eq(9) then, refers to the *total* velocity component.

Figure 10 shows the results of this analysis. Plotted on the longitude-latitude section are the seasonal total (mean plus perturbation) zonal velocity components at every 20° of longitude. The shaded regions indicate zones of easterly ( $u < 0$ ) winds. Superimposed upon the zonal wind distribution are isopleths of the gradient of absolute vorticity defined in eq (9). Only values greater than zero are plotted, and these values appear as elongated regions that vary in intensity and position from season to season. The scales of all quantities are indicated on the figure.

Regions where the gradient of absolute vorticity exceeds zero are regions of energy source for small-scale transient disturbances, which in turn interact with the mean flow and allow a continuing energy exchange. As described by Colton (1973), such disturbances act as important dissipation mechanisms of the ultralong wave energy generated by the large-scale forcing. The most predominant region is that associated with the large shear on the poleward side of the easterly maximum of the Eastern Hemisphere, although it is seen to extend across Africa in all seasons except SON. With the movement of the easterly jet northward during the Northern Hemisphere summer, the unstable band extends over northern India from the western Pacific and westward to the Atlantic Ocean. With the weakening of the systems in SON, the regions of instability are diffuse and weaker. However, at low latitudes in all seasons, there are preferred regions determined by the positions of the forced ultralong stationary waves for the development of upper tropospheric transient waves at the expense of the mean seasonal forced flow.

Note that most of these regions correspond to location points of disturbances which later became tropical storms, as determined observationally by Gray (1968). The major

differences occur over the continental regions of Africa and Brazil, which (although not centers of tropical storms) are highly disturbed regions.

## 6. LONGER TERM VARIATIONS

One of the most important and interesting aspects of this study is the determination of the physical makeup of the correlations found by Walker (1923) between distant low-latitude station pairs. To inquire into this problem, we will examine the seasonal variation of various quantities from the annual mean, which is defined by the average of the seasonal distributions determined by the model.

We emphasized in earlier sections of this paper that the seasonal response is a function of many factors including the basic flow and the extent of the easterlies, the position of the heating and orographic forcing relative to the basic flow, and the magnitude of the forcing, all of which vary seasonally. The variation in phase and magnitude of the modes of largest response at 25°N, 0°, and 25°S are shown in figures 11A, 11B, and 11C, respectively. On the plot for each wave are the numerals 1, 2, 3, and 4, which identify the phase-kinetic energy coordinates for that particular mode for the seasons DJF, MAM, JJA, and SON, respectively. The scale for figure 11C is increased by a factor of 20 because of the relatively weak response in the Southern Hemisphere. In the equatorial region, only the phase and magnitude of the  $s=1$  mode is shown since the response of the other modes is at least an order of magnitude less (fig. 6). Figure 11A shows a large variation of both phase and latitude of the  $s=1$  mode with magnitude peaks in MAM and JJA but with a phase difference over 60° of longitude. The  $s=2$  mode shows less variation in magnitude but a wide range in phase. The peaks in JJA in the  $s=1$  and 2 modes are nearly in phase and represent the long-period Rossby waves responding to the seasonally varying forcing field and basic field. The diagram for the equatorial zone (fig. 9B) indicates a very large amplitude response in MAM with only a 30° phase difference between DJF and MAM. This is the ultralong Kelvin wave trapped about the Equator responding to the slowly varying forcing field within the easterly wind regime. The southern section (fig. 11C) shows only a weak response but with very large phase differences.

In figure 11, the variations in phase and amplitude as a function of latitude are complicated; thus, trying to determine simultaneous variations between the zones is a difficult task. Another possibility is to follow the work of Walker and calculate correlations between station pairs or (in our model) between gridpoint pairs. The calculation of the correlation coefficient  $R$  of some quantity  $P(x,y)$  with a standard quantity  $P_s(x_s,y_s)$  situated at  $(x_s,y_s)$  over a period of time may be defined by

$$R(x,y) = \frac{\sum_i A_i(x,y) B_{si}(x_s,y_s)}{\sqrt{\sum_i A_i^2(x,y) B_{si}^2(x_s,y_s)}} \quad (10)$$

where

$$A_i = P_i(x,y) - \bar{P}(x,y)$$

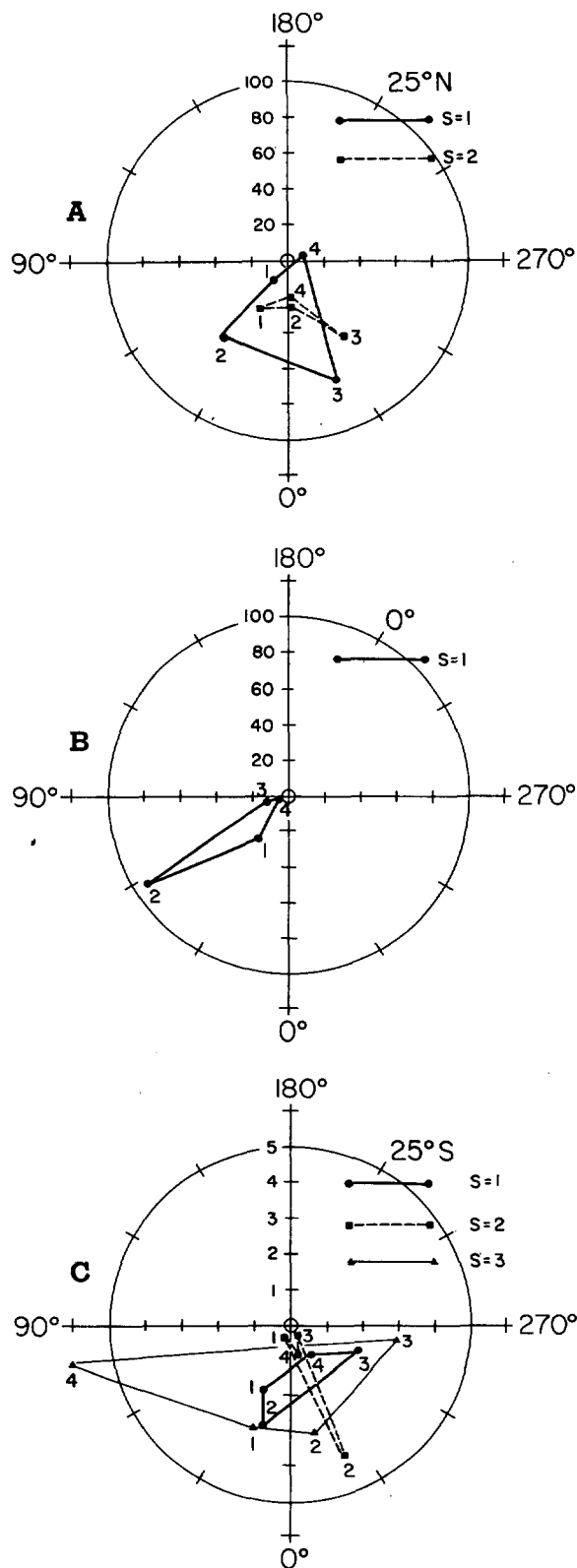


FIGURE 11.—Phase/amplitude characteristics of the kinetic energy response at (A) 25°N, (B) 0°, and (C) 25°S. The longitudinal waves plotted are shown on each figure, and the numerals 1, 2, 3, and 4 refer to the phase/amplitude coordinate in DJF, MAM, JJA, and SON, respectively.

and

$$B_{s,i} = P_{s,i}(x_s, y_s) - \bar{P}_s(x_s, y_s).$$

The subscript  $i$  denotes the observation of  $P(x, y)$  at time  $i$ . In our model,  $i$  may take on values 1 through 4 thus

taking into account the four seasonal estimates of an array  $P(x, y)$  produced by the model.  $\bar{P}(x, y)$  is the time-means of  $P_i(x, y)$  over the annual period so that  $A_i$  and  $B_{s,i}$  denote deviations from their respective time-means.

Figures 12A and 12B show two examples of the fields of  $R(x, y)$  providing the correlations between the seasonal variation of  $P(x, y)$  from the annual mean  $\bar{P}(x, y)$  with similar quantities at  $(x_s, y_s)$ . The shaded regions denote negative correlations. The quantity chosen to perform the correlations was the geopotential  $\phi_2(x, y)$  at the lower level (750 mb) of the model. This is the closest analog possible from the model to Walker's southern oscillation index, which (according to Troup 1965) was essentially the surface pressure. Two standard locations were chosen, a gridpoint near Djakarta and another near Bombay. Both diagrams signify roughly the same distribution of  $R(x, y)$ , which infers that the Eastern Hemisphere possesses an anomalously high geopotential at 750 mb while most of the Western Hemisphere has anomalously low geopotential. Also, the western and eastern Pacific regions show extremes in  $R(x, y)$  in the very location of the Walker circulation as defined by Bjerknes (1969). Most importantly, the results are strikingly similar to those of Troup (1965) who found that station-pair correlations based at Djakarta indicated anomalously low surface pressure in the Eastern Hemisphere in conjunction with anomalously high surface pressures in the Western Hemisphere.

To use these results to infer the physics behind Walker's correlation, we first have to understand the main differences between Walker's *station-pair* correlations and the model's *gridpoint* correlations. The basic difference resides within the data used. Walker made his estimates using many years of data; his correlations refer to anomalies about various climatic averages derived from the long data records at his various station pairs. He used such data to calculate monthly, seasonal, and annual correlations. This means that he calculated the mean value of a parameter over a particular time period in a given year and calculated its anomaly from the climatic average before proceeding to the station-pair correlations. Our estimates differ in that we have only one annual mean, which would also be the model climatic mean, and the four cases, DJF, MAM, JJA, and SON that together constitute this annual mean. Therefore, if we assume that this seasonal variation continues year after year, the climates and the individual seasonal averages would remain the same, which insists that all correlations made on a monthly, seasonal, or annual basis following the method of Walker would result in a perfect correlation at all points, producing meaningless results. Thus, as we are unable to duplicate Walker's experiment exactly, we seek correlations of gridpoint pair deviations from the annual mean of each season to give the distributions of  $R(x, y)$  shown in figure 12. Such distributions are seen to signify the interdependence of all the tropical atmosphere and show the effect of an anomaly occurring in one region and how it will influence other regions by the communication of the forced ultralong waves described in the preceding sections.

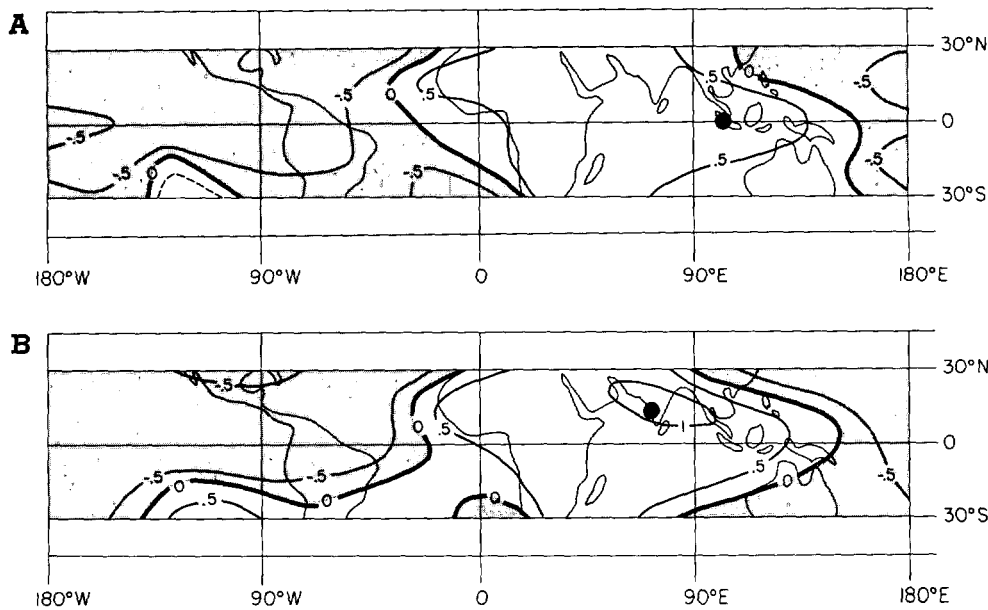


FIGURE 12.—Distributions of the correlation coefficient  $R(x,y)$  for the seasonal anomalies of the geopotential,  $\phi_2$ , relative to the anomalies at (A) Djakarta, Indonesia, and (B) Bombay, India, each denoted by a solid circle. The shaded regions denote negative correlation coefficients.

Specifically, then, it appears that the correlations of Walker and others are no more than variations in the magnitude of the response of the ultralong slow-moving waves of low latitudes. For example, a strong monsoon in JJA over the Indian region may be expected to provide a hemispheric response. Similarly, we have noted that the eastern and western Pacific Ocean are exactly out of phase in the correlation coefficient or in the anomalous seasonal geopotential at 750 mb. In other words, when the pressure is low in the west, it is high in the east. This can be seen from the large  $s=1$  Kelvin wave response at low latitudes, meaning that, if the net heating increases in the region of activation of the wave, the whole tropical atmosphere must respond correspondingly. In this manner the Bjercknes (1969) picture of Walker circulation may now be thought of as the Kelvin wave response to seasonally varying forcing, and Walker's correlations may be considered to be further deviations (e.g., stronger heating or cooling) superimposed upon these regular seasonal anomalies. Whereas the above model proposes a mechanism of atmospheric teleconnection at low latitudes, it does not pretend to explain how the anomaly itself is produced.

## 7. CONCLUDING REMARKS

This paper is the third in a continuing study of the stationary forced waves in low latitudes. The results presented in W1 and W2 have been extended to include the equinoctial seasons, which were shown to exhibit large differences compared to both solstitial seasons and also to the expected symmetry between themselves. That is, the transition from the Northern Hemisphere summer to winter is very different from the reverse transition at low latitudes.

The seasonal response was studied so as to infer possible relationships between the seasonal mean flow and cir-

culations of periods much less and much greater than the few months constituting the seasonal average. We pointed out that there were regions in which energy from the seasonal mean flow (basic plus perturbation) was available for the development of transient phenomena due to the barotropic instability of the basic state and that such regions agree fairly well with the geographic locations of tropical storms as observed by Gray (1968). Furthermore, it was possible to identify the ultralong period variations of low latitudes, identified by Walker (1923), as small variations in the regular quasi-stationary forced seasonal waves.

One of the most interesting features of the low-latitude response was the individuality of the forced flow within and without the easterly channel of the basic flow. This allowed the interpretation of the Walker circulation as a forced Kelvin wave more sensitive to the long-wave forcing than to short-wave excitation. Its phase/amplitude distribution (fig. 11B) shows that the main variability exists in its amplitude while the nearly constant phase corresponds to an ascending leg over Indonesia with descending air over the eastern Pacific Ocean. Krishnamurti (1971a) described this cell as merely a southern extension of the much stronger Indian summer monsoon system. However, we have shown that these two systems are nearly independent for the time scales we are considering, with the monsoon system as a Rossby-type response separated from the equatorial Kelvin wave by the critical latitude. Furthermore, the Kelvin wave shows a maximum amplitude in MAM (fig. 11B) while Krishnamurti (1971a) only sensed the Walker circulation during JJA, a time when the monsoonal forcing dominates the subtropics but when long-wave forcing about the Equator is small. Thus on a seasonal basis, each circulation appears as an individual entity.

Finally, it is interesting to speculate on the relevance of this study to the observed 40- to 50-day periodicity of the tropical atmosphere noted by Madden and Julian (1972). Using long time series upper atmospheric data in the low latitudes, they observed a mean wave (with the preceding period and of low longitudinal wave number and generally restricted in latitude extent) to lie between 10°N and 10°S. Furthermore, the observations suggest that the oscillation is the result of the eastward propagation of large-scale zonal circulations. The discussion in section 4 of this paper suggests that Madden and Julian probably were sensing the slow movement of the low-latitude Kelvin wave response, which (as we have seen) manifests itself as a long-wave zonal circulation. However, it is not possible within the confines of this study to explain the 40- to 50-day period with only seasonal forcing functions (~ 90-day period). The effect of shorter term forcing at low latitudes is being studied in an attempt to explain the Madden-Julian periodicity.

#### ACKNOWLEDGMENTS

This work was supported by the Atmospheric Science Section of the National Science Foundation under Grant GA-31694.

I would like to thank Beverly Gladstone for drafting the figures.

#### REFERENCES

- Bjerknes, Jakob, "Atmospheric Teleconnections From the Equatorial Pacific," *Monthly Weather Review*, Vol. 97, No. 3, Mar. 1969, pp. 163-172.
- Colton, Donald E., "Barotropic Scale Interactions in the Tropical Troposphere During the Northern Summer," *Journal of the Atmospheric Sciences*, Vol. 30, No. 7, Oct. 1973, pp. 1287-1302.
- Gray, William M., "Global View of the Origin of Tropical Disturbances and Storms," *Monthly Weather Review*, Vol. 96, No. 10, Oct. 1968, pp. 669-700.
- Katayama, A., "On the Heat Budget of the Troposphere Over the Northern Hemisphere," Ph.D. thesis, Tohoku University, Japan, Jan. 1964, 264 pp.
- Kidson, John W., "The General Circulation of the Tropics," Ph.D. thesis, Department of Meteorology, Massachusetts Institute of Technology, Cambridge, Mass., Sept. 1968, 205 pp.
- Kidson, John W., Vincent, Dayton G., Newell, Reginald E., "Observational Studies of the General Circulation of the Tropics: Long Term Mean Values," *Quarterly Journal of the Royal Meteorological Society*, Vol. 95, No. 404, London, England, Apr. 1969, pp. 258-287.
- Koteswaram, P., and George, C. A., "On the Formation of Monsoon Depressions in the Bay of Bengal," *Indian Journal of Meteorology and Geophysics*, Vol. 9, No. 1, New Delhi, Jan. 1958, pp. 9-22.
- Krishnamurti, T. N., "Tropical East-West Circulations During the Northern Summer," *Journal of the Atmospheric Sciences*, Vol. 28, No. 8, Nov. 1971a, pp. 1342-1347.
- Krishnamurti, T. N., "Observational Study of the Tropical Upper Tropospheric Motion Field During the Northern Hemisphere Summer," *Journal of Applied Meteorology*, Vol. 10, No. 6, Dec. 1971b, pp. 1066-1096.
- Lorenz, Edward N., "Barotropic Instability of Rossby Wave Motion," *Journal of the Atmospheric Sciences*, Vol. 29, No. 2, Mar. 1972, pp. 258-264.
- Madden, Roland A., and Julian, Paul R., "Description of Global-Scale Circulation Cells in the Tropics With a 40-50-Day Period," *Journal of the Atmospheric Sciences*, Vol. 29, No. 6, Sept. 1972, pp. 1109-1123.
- Manabe, Syukuro, Holloway, J. Leith, Jr., and Stone, Hugh M., "Tropical Circulation in a Time-Integration of a Global Model of the Atmosphere," *Journal of the Atmospheric Sciences*, Vol. 27, No. 4, July 1970, pp. 580-613.
- Montgomery, R. B., "Report on the Work of G. T. Walker. Reports on Critical Studies of Methods of Long-Range Weather Forecasting," *Monthly Weather Review Supplement* No. 39, Apr. 1940, pp. 1-22.
- Nitta, Tsuyoshi, and Yanai, Michio, "A Note on the Barotropic Instability of the Tropical Easterly Current," *Journal of the Meteorological Society of Japan*, Vol. 47, No. 2, Tokyo, Japan, Apr. 1969, pp. 127-130.
- Taylor, V. Ray, and Winston, Jay S., "Monthly and Seasonal Mean Global Charts of Brightness from ESSA 3 and ESSA 5 Digitized Pictures, Feb. 1967-Feb. 1968," *ESSA Technical Report NESC 46*, National Environmental Satellite Center, U.S. Department of Commerce, Washington, D.C., Nov. 1968, 9 pp.
- Troup, A. J., "The Southern Oscillation," *Quarterly Journal of the Royal Meteorological Society*, Vol. 91, No. 390, London, England, Oct. 1965, pp. 490-506.
- Walker, Gilbert T., "Correlation in Seasonal Variations of Weather, VIII. A Preliminary Study of World Weather," Vol. 24, Part 4, Superintendent of Government Printing, Calcutta, India, 1923, pp. 75-131.
- Webster, Peter J., "Response of the Tropical Atmosphere to Local, Steady Forcing," *Monthly Weather Review*, Vol. 100, No. 7, July 1972, pp. 518-541.
- Webster, Peter J., "Remote Forcing of the Time-Independent Tropical Atmosphere," *Monthly Weather Review*, Vol. 101, No. 1, Jan. 1973, pp. 58-68.

[Received June 29, 1973; revised September 11, 1973]